Influence of UV irradiation on the skin-immune cell inflammatory response

Rebecca Miceli
Rensselaer Polytechnic Institute
Noah Allen
Rensselaer Polytechnic Institute
Meaghan Jankowski
Rensselaer Polytechnic Institute
Jennifer Haghpanah
Estée Lauder (United States)
Rishabh Kala
Estée Lauder (United States)
Jennifer Hurley
Rensselaer Polytechnic Institute
Jonathan Dordick
dordick@rpi.edu

Rensselaer Polytechnic Institute

Article

Keywords:

Posted Date: May 20th, 2026

DOI: https://doi.org/10.21203/rs.3.rs-9439427/v1

Additional Declarations: No competing interests reported.

Abstract

Human skin serves as the first line of defense against ultraviolet radiation (UVR) light. UVR is known to cause cellular and extracellular damage to skin when left unprotected, causing inflammation due to the overproduction of intracellular reactive oxygen species (iROS) and pro-inflammatory cytokines. Herein, we utilize keratinocytes (HaCaT cells), and THP-1 monocytes transformed into Langerhans-like cells (LC) and circulating macrophages (THP1-PMA) to recreate the epidermal and dermal layers of the skin. We first established a baseline for cellular reaction to UVR, quantifying cell viability, iROS, and cytokine production 24 h post-exposure to SHAM, 10 J/cm^2 UVAR, and/or 500 mJ/cm^2 UVBR. Next, we then applied an inhibitor of nicotinamide adenine dinucleotide phosphate oxidase subunit 2 (NOX2), GSK2795039 (GSK), to determine whether NOX2 inhibition can reduce iROS and pro-inflammatory cytokines 24 h post-UVR exposure. GSK significantly reduced the inflammatory response in monolayer and co-culture systems, including a 3-fold reduction in iROS production in the epidermis model following exposure to UVAR+UVBR compared to non-GSK treated cells. To our knowledge, this is the first time that GSK has been studied to inhibit ROS overproduction after UVR in a complex skin-immune system.

Introduction

Skin is the largest organ of the body and serves as the first line of protection against pathogens, harmful chemicals, and ultraviolet radiation (UVR) light[1,2]. Human skin is composed of three main layers – the epidermis, dermis, and hypodermis[3]. The epidermis is an avascular outermost layer, ~ 0.5 to 1.5 mm thick[1,4], consisting of mainly keratinocytes (skin cells) and Langerhans cells (dendritic immune cells)[5]. The second layer of skin, the dermis, is ~ 2 to 4 mm thick, and includes circulating macrophages[1,5,6]. Together these layers work in concert to form the complex skin-immune system to provide protection against external factors such as UVR[3,7–9].

When cells of the epidermis are negatively compromised, such as by UVR, keratinocytes and Langerhans cells (LC) release cytokines, which activate the host immune system[10]. Though poor at phagocytosis, LC secrete a number of cytokines, including IL-1β and IL-6 when stimulated, thus initiating a cutaneous cellular immune responses[3,11]. The dermal layer contains circulating macrophages, which can be in the pro-inflammatory (M1) or anti-inflammatory (M2) state[12,13]. In the M1 phase, macrophages release cytokines IL-1β, TNFα, and IL-6, and in the M2 phase, cytokines IL-10, IL-12, and TNFβ are released [12]. Keratinocytes can release IL-1α and IL-1β under inflammatory stress[14]. UVR is known to cause acute injury to both the epidermis and dermis of human skin, through sunburn, inflammation, and photo-immunosuppression, which activate the skin-immune system[15].

UVR is subdivided into three wavelength bands of increasing energy: UVA (320–400 nm), UVB (280–320 nm), and UVC (100–280 nm)[15]. UVR consists of ~ 95% UVA radiation (UVAR), and ~ 5% UVB radiation (UVBR); UVC radiation (UVCR) does not reach the Earth's surface[16]. Humans are exposed to differing levels of UVR daily depending on latitude, altitude, skin exposure time, weather, time of day, and

season[15,17,18]. Repeated or high-dose exposures to UVR can cause cellular and extracellular damage to human skin when left unprotected, including an overproduction of pro-inflammatory cytokines (IL-1α, IL-1β, and IL-6) potentially triggering damage to the surrounding tissue through cellular senescence and accelerating cellular aging[19–21]. UVR also causes the release of reactive oxygen/nitrogen species (ROS/RNS), such as hydrogen peroxide, superoxide, hydroxyl radical, and peroxynitrite[22–24].

Inhibitors of nicotinamide adenine dinucleotide phosphate (NADPH) oxidases (NOXs) have been studied for their potential use in blocking ROS production[25]. Specifically, the NOX2 isoform, primarily expressed in neutrophils and macrophages, is responsible for superoxide production and subsequent ROS generation[26]. While complete loss-of-function is detrimental to humans, excess production of ROS from NOX2 activity can result in increased inflammation, suggesting that selective NOX2 inhibition may be beneficial in modulating acute inflammatory responses[26]. Korkmaz et al., 2020, showed that NOX2 expression is increased in keratinocytes following a sunburn event, producing large amounts of ROS and triggering an inflammation cascade. Therefore, we propose that NOX2 inhibition will decrease skin damage caused by UVR through reduction of oxidative stress and inflammation, protection of DNA, and prevention of cell death[27,28]. Additionally, inhibition of NOX2 may prevent premature skin aging, as skin inflammation is known to cause a breakdown of collagen and elastin[29]. GSK2795039 (GSK) is a selective inhibitor of NOX2, shown to inhibit ROS production in BV2 microglial cells[30], HaCat cells[28], and neutrophils[31]. GSK acts on NOX2 as a competitive, reversible inhibitor of NADPH binding to $cytb_{558}$ [30]. To our knowledge, this is the first time that GSK has been studied to inhibit ROS overproduction after UVR in a basic and complex skin-immune system.

Herein, we explored the creation and use of two skin-immune systems; an epidermis model consisting of HaCaT and LC cells, and a dermis model, which adds circulating macrophages to the epidermis model. Using doses of 10 J/cm^2 UVAR and/or 500 mJ/cm^2 UVBR, we studied the impact of UVR on an inflammatory response through cell viability, ROS production, and cytokine production, and the effect of GSK on reducing the inflammatory response.

Results

1. Design and Assembly of Skin-Immune Cell Culture Systems

UVR has differing degrees of skin penetration; UVAR can penetrate both epidermal and dermal layers, but UVBR only penetrates the epidermis (Fig. 1A**).** To effectively study the effects of UVR on skin, we developed multiple cell culture systems compatible with 96-well plates. A simple monoculture of each cell line (HaCaT, LC, THP1-PMA) (Fig. 1B**)**, was first used as a baseline for the effect of UVR on cell viability and inflammatory response. THP1-PMA cells were differentiated from THP-1 monocytes using PMA **(Supplemental Fig. 1)**, and LC cells were differentiated from THP-1 monocytes using GM-CSF, IL-4, and TFGβ **(Supplemental Fig. 2)**. Next, two complex skin-immune models were created; a traditional co-culture of HaCaT cells and LC cells in direct contact, which represented the epidermis (Fig. 1C**)**, and a

dermis model (Fig. 1D) upon addition of THP1-PMA macrophages via a transwell co-culture to the epidermis model. Treatment consisted of no UVR (SHAM, Fig. 1E), UVBR only (Fig. 1F), or UVAR+UVBR (Fig. 1G).

2. Determining appropriate UVR doses on monocultures

Monolayers were used to determine baseline effects of differing levels of UVR on the skin-immune cells. Each cell line was dosed with UVAR and/or UVBR and returned to 24 h of incubation (recovery) prior to cell viability and cytokine production assays. THP1-PMA cells were only dosed with UVAR, as they reside in the dermal layer. HaCaT cells were dosed with 0–850 mJ/cm^2 of UVBR, where ~ 25% reduction in cell viability (Fig. 2A) and a 3-fold increase in pro-inflammatory IL-6 (Fig. 2B) was observed at 500–850 mJ/cm^2 compared to SHAM cells. Similarly, LCs had ~ 50% cell viability reduction (Fig. 2C) and significantly increased cytokine production for IL-4, TNFα, and IL-1β (Fig. 2D) in doses > 100 mJ/cm^2 of UVBR compared to SHAM. Based on monoculture results, a dose of 500 mJ/cm^2 was selected for further experiments. HaCaT cells (Fig. 2E, F), THP1-PMA cells (Fig. 2G, H), **and** LCs (Fig. 2I, J), and all had a high tolerance to UVAR with non-significant cell death and cytokine production, respectively, up to 10 J/cm^2. Based on viability and cytokine production, we selected the maximum UVAR dose of 10 J/cm^2 for further experiments.

3. Epidermis co-culture model is more physiologically reactive to UVR compared to cells in monoculture.

After doses of 500 mJ/cm2 UVBR and 10 J/cm2 UVAR were established, cell viability and iROS levels were investigated in the monocultures, and epidermis and dermis co-culture systems. In monoculture, HaCaT cells were significantly impacted by exposure to UVBR alone and in combination with UVAR, where cell viability decreased 50% and 20%, respectively (Fig. 3A, **orange)**. Immune cells in monoculture were not significantly impacted by exposure to UVR (THP1-PMA, Fig. 3A **pink**) (LC, Fig. 3A **green**). In the epidermis co-culture system, UVR induced ~ 10% cell reduction compared to SHAM (Fig. 3B), differing from the HaCaT monoculture results. In the dermal transwell model, the epidermal layer exposed to UVR had a decreased viability compared to SHAM, ~ 60% cell reduction, differing from the epidermis co-culture without the THP1-PMA cells in transwell (Fig. 3C, **brown**). THP1-PMA cell viability was significantly reduced when UVR was added to the system, ~ 40% cell reduction compared to SHAM, differing from their monoculture response to UVR (Fig. 3C, **pink)**.

iROS normalized to cell viability was also assessed in all systems. In their monocultures, HaCaT cells expressed a 2.2- and 2.0-fold increase in iROS when exposed to UVBR alone and UVAR+UVBR, respectively, compared to SHAM (Fig. 3D, **orange)**. iROS production was not significantly altered in THP1-PMA cells after UVR exposure (Fig. 3D, **pink)**, and LC cells produced significantly less iROS when exposed to UVR compared to SHAM (Fig. 3D, **green**). In the epidermis cell system, iROS levels increased

2-fold with UVBR, and 3-fold with the addition of UVAR, compared to SHAM levels, showing a compounding effect of UVR on the epidermis system (Fig. 3E). In the dermis model, we observed a 2-fold increase in iROS production with the addition of UVBR in the epidermal cell layer compared to SHAM; however, we did not observe the additional iROS production from UVAR, as observed in the epidermis model without transwell THP1-PMA (Fig. 3F, **brown**). In the THP1-PMA cells, we observed a 2.4-fold (UVBR epidermis exposure) and 2.0-fold (UVAR+UVBR system) increase in iROS production (Fig. 3F, **pink**).

4. Cytokine responses are altered for cells in complex skin-immune co-culture systems compared to monocultures, 24 h post-UVR.

We proceeded to investigate eight cytokines selected for their known involvement in the skin-immune system and reaction to UVR [23,32–36], using only SHAM and the physiologically relevant UVAR+UVBR model, simply referred to the UVR model in this section (Fig. 4). Pro-inflammatory cytokines IL-1β (Fig. 4A) and IL-5 (Fig. 4B), were significantly reduced in all models except the HaCaT monoculture 24 h post-UVR exposure. Pro-inflammatory IFNγ was significantly reduced in HaCaT and THP1-PMA monocultures and the dermis model, where LC monocultures secreted approximately 6-fold higher concentrations of IFNγ compared to HaCaT and THP1-PMA monocultures (Fig. 4C). Pro-inflammatory IL-6 was significantly produced in all cell models containing HaCaT cells but significantly decreased in THP1-PMA and LC monocultures (Fig. 4D). Relatively low levels of TNFα were produced, with mixed significance depending on cell/model type (Fig. 4E). IL-2 was also produced in low levels, > 10 pg/mL, and was significantly reduced in the epidermis and dermis models in UVR vs. SHAM groups (Fig. 4F). Anti-inflammatory IL-10 was secreted significantly more in the UVR HaCaT cell monoculture compared to SHAM and produced significantly less in all models containing immune cells (Fig. 4G). Anti-inflammatory IL-4 was significantly reduced, ~ 4-fold less, in the UVR epidermis model compared to SHAM (Fig. 4H).

5. NOX2 inhibition significantly reduces the production of iROS after UVR exposure

The production of iROS in HaCaT cells and immune cells in response to UVR suggests that a reduction in iROS may protect these cells from UVR-induced oxidative damage. NOX2 is a major source of iROS in macrophages[26,30] and is known to be present in HaCaT cells [28]. Moreover, NADPH-oxidases are partially responsible for ROS production in cells after introduction to a stressor, such as UVR[37,38], and is involved in the immune system and inflammation[39]. Thus, inhibition of NOX2 may result in the protection of skin-immune cell function from UVR-induced damage. To this end, we used a promising NOX2 inhibitor, GSK2795039 (GSK), and tested its ability to reduce iROS production after exposure to UVR. A preliminary dose response was generated in HaCaT monocultures dosed with UVAR+UVBR, where cell viability and iROS are shown in **Supplemental Fig. 3.** Based on these results, we selected 8 μM GSK for subsequent NOX2 inhibition studies. Cells were seeded and incubated with 8 μM GSK, 48 h prior to UVR. After

incubation, cells were exposed to UVAR and/or UVBR then, media was replaced with fresh media including 8 μM GSK.

Cell viability and iROS production normalized to cell viability were measured after GSK treatment for the monocultures, and epidermis and dermis co-culture systems after 24 h of incubation post-UVR (Fig. 5). The addition of GSK had a minor effect on cell viability, inducing a minor increase in cell viability in the HaCaT monoculture UVBR group compared to non-GSK treated (Fig. 5A), a decrease in the SHAM epidermis (Fig. 5B), and minor viability changes in the dermis culture (Fig. 5C). All iROS data has been normalized to cell viability. All monocultures showed a significant reduction in iROS production in all GSK treated cells compared to their respective non-GSK treated levels (Fig. 5D). Notably, UVR treated HaCaT cells had ~ 2.0-fold decrease in iROS compared to non-treated UVR cells, down to levels similar to basal (Fig. 5D, **orange**). In the epidermis co-culture system, iROS was significantly reduced in all groups, including a 3.7-fold decrease in iROS for UVAR+UVBR treated cells compared to non-GSK treated, irradiated cells (Fig. 5E). In the dermis co-culture system, the epidermis portion followed the same trend as shown in Fig. 5E; however, total iROS levels were lower compared to the epidermis co-culture without THP1-PMA cells (Fig. 5F, **brown).** The THP1-PMA cells in transwell produced significantly less iROS in groups treated with GSK compared to those without GSK; however, the overall iROS levels were higher in the transwell system compared to their respective monoculture results (Fig. 5F, **pink).**

6. Assessment of the NOX2 inhibitor, GSK, on cytokine expression in the complex skin-immune model, 24 h post SHAM or UVAR+UVBR exposure.

We further investigated if GSK could significantly impact cytokine production in the complex skin-immune model after exposure to UVAR+UVBR. Following 48 h pre-treatment, and subsequent 24 h post-treatment of the complex skin-immune model with 8 μM GSK, cytokine production was significantly impacted in specific cell systems (Fig. 6). For example, levels of pro-inflammatory cytokines IL-1β (Fig. 6A), and IL-5 (Fig. 6B) were significantly higher in GSK treated HaCaT monocultures compared to non-GSK treated, SHAM cells. TNFα production was significantly decreased in HaCaT UVR monocultures compared to non-GSK treated cells, and significantly increased in THP1-PMA monocultures exposed to UVAR (Fig. 6C). Results for IL-2 (Fig. 6D) were similar to those described for IL-5. Anti-inflammatory IL-10 was significantly produced in HaCaT SHAM monocultures, THP1-PMA UVAR monocultures, and the epidermis co-culture model exposed to UVR (Fig. 6E**).** Additionally, anti-inflammatory IL-4 was only significantly produced in the epidermis co-culture exposed to UVR, however there was ~ 5.0-fold decreased IL-4 secretion in UVR treated epidermal cells vs SHAM (Fig. 6F). Data for IFNy and IL-6 are shown in **Supplementary Fig. 4**, where GSK did not significantly impact cytokine secretion in any cell or model type.

Discussion

Herein, we explored the creation and use of skin-immune systems to elucidate the inflammatory response of a skin model to UVR by assessing cell viability, iROS production, and cytokine expression. An

epidermis model was created through the traditional co-culturing of HaCaT cells and LC, differentiated from THP-1 monocytes, and a dermis model was created through the addition of THP1-PMA macrophages added via transwell-insert to the epidermis model. Finally, we added a NOX2 inhibitor, GSK, to each skin-immune system to investigate how inhibition of NOX2 can reduce the inflammatory response of skin from UVR.

Extended skin exposure to UVR can lead to the breakdown of collagen and elastin, DNA damage, and inflammation, leading to premature skin aging[7,21,29]. Here, we focus on sunburn, an acute inflammatory condition affecting the skin from UVR exposure [40]. First, we used cell viability and iROS production measurements to understand the baseline effect on our skin-immune model. HaCaT cells and LC in monocultures demonstrated a significant inflammatory response to 500 mJ/cm^2 UVBR, as it generated ~ 40% cell death in HaCaT cells and ~ 60% cell death in LC cells, with an increase in pro-inflammatory cytokines IL-6 and TNFα for HaCaT cells and an increase in IL-4, TNFα, and IL-1β in LC cells. Indeed, 500 mJ/cm^2 UVBR is known to produce a strong inflammatory response in the skin[41–43]. UVBR has been shown to affect cell viability through the initiation of apoptosis and necrosis, and subsequent failure to proliferate. Therefore, reductions in cell viability are driven in part by an increase in ROS[2,23,40,44]. In addition, a UVAR dose of 10 J/cm^2 was chosen based on its moderate response in THP1-PMA and LC cells, and significant increase in pro-inflammatory cytokines IL-1β and IL-6. Our results matched those of Chiarelli-Neto et al., 2023, who reported a significant increase in inflammatory markers such as ROS in mouse macrophage J774 cells after 12 J/cm^2 UVAR, and Valencia and Kochevar (2006), who reported an inflammatory response in keratinocytes immediately after a dose of 10 J/cm^2 UVAR[23,45].

Interestingly, the addition of UVAR to the HaCaT monoculture system rescued cell viability compared to UVBR alone in the monoculture and traditional co-culture. This result may be explained by the wound healing effects of low doses of UVAR[19,20]. Low doses of UVAR, including a dose of 10 J/cm^2, are given to patients during phototherapy[19,20]. Leong et al.[46] found that low dose UVAR induced the release of the anti-inflammatory cytokine IL-4 in keratinocytes and dendritic cells. Increased IL-4 secretion was hypothesized to cause benefits to skin, including reduced ROS damage, less disruption of mutated keratinocytes, and epidermal thickening [46]. Indeed, when our HaCaT cells were exposed to increasing levels of UVAR, there was an increase in IL-4 production moving from 3 J/cm^2 to 10 J/cm^2, which may explain recovery in cell viability after combined exposure to UVAR+UVBR.

In our complex skin-immune system, immune cell viability was not significantly impacted by UVAR and/or UVBR. Our epidermis model showed moderate cell viability reduction with UVAR and/or UVBR; however, the same epidermis model within the dermis transwell system resulted a 40% reduction in cell viability, closely mimicking the results of the HaCaT cell monoculture. Results from the epidermis model are supported by Ortner et al., 2024,[9] who noted that LC may by resistant to DNA damage induced from UVR through rapid repair of DNA double-strand breaks, and subsequent protection of keratinocytes after UVR damage. Additionally, UVR has been shown to activate LC-mediated phagocytosis of damaged keratinocytes, thus reducing the inflammatory effects of sunburn[47]. Interestingly, the LC-driven

protection seen in the epidermis model disappears when THP1-PMA macrophages are added to the system. After THP1-PMA macrophages are exposed to UVAR, they undergo oxidative stress, generating ROS and secreting pro-inflammatory cytokines, which ultimately shifts them into a pro-inflammatory (M1) phenotype[13]. The differences in cell viability response between the epidermis co-culture and the dermis transwell co-culture justify the inclusion of both systems in our study. Further studies are necessary to understand the negative impact THP1-PMA macrophages have on the protective epidermis co-culture of keratinocytes and LC.

One of the major causes of inflammation from sunburn is the accumulation of ROS [2,15,23,40,44]. Known to cause damage to lipids, proteins, and DNA, ROS and RNS produced from UVR include superoxide, peroxynitrite, and hydroxyl radicals[23,48,49]. We measured intracellular ROS production using DCFDA, a cell permeable probe that is sensitive to oxidative stress [50]. As expected, HaCaT cells produced significantly more iROS in UVR treated cell compared to SHAM; however, THP1-PMA and LC cells in monoculture did not produce significantly more iROS compared to their respective SHAM cultures. In the epidermis culture, iROS levels showed 2-fold and 3-fold increases over SHAM for UVBR alone and UVAR+UVBR, respectively, indicating that co-cultured HaCaT + LCs shows a more physiologically relevant reaction to UVR compared to monocultures. Chettouh-hammas et al., 2023, reported a similar result, where monocultured cells showed a lower inflammatory response compared to the same co-cultured cells as a reconstructed human epidermis. Thus, lack of iROS produced by LC and THP1-PMA cells in monoculture, and a subdued response from HaCaT cells in monoculture, may be expected.

Cytokines are secreted in the skin after sunburn, and therefore, we analyzed eight different cytokines in our complex skin-immune model, 24 h post SHAM or UVR exposure. Pro-inflammatory cytokines IL-1β, IFNy, and IL-5 were significantly reduced in UVAR+UVBR treated cells vs SHAM, and IL-6 was significantly reduced in THP1-PMA and LC macrophages. We expected pro-inflammatory cytokines to increase after UVR. However, this was only observed for IL-6 secretion in the cell models containing HaCaT cells. Our anti-inflammatory cytokine IL-10 significantly increased in HaCaT monocultures but decreased in THP1-PMA macrophages and LC monocultures, and the epidermis model, in contrast to our expectation that both pro-and anti-inflammatory cytokine secretion to be significantly increased at 24 h post-UVR. Some literature suggests that pro-inflammatory cytokines may peak outside of our 24 h timepoint, such as Scordi and Vincek, 2000, who showed that IL-6 peaked at both 6 h and 48 h, IL-2 and IL-10 peaked at 72 h, and IL-1β peaked at 48 h post irradiation.

After capturing cell viability, iROS, and cytokine production associated with each cell model, we applied GSK to our system. GSK is a selective NOX2 inhibitor, used to block the production of superoxide in our skin-immune systems after UVR exposure[39]. NOX2 is primarily expressed in neutrophils and macrophages[38,53]. While loss of function can be detrimental to an organism, the chronic activation of NOX2 can lead to inflammation and tissue damage[39]. NADPH oxidases are a superfamily of enzymes that generate ROS. By blocking this process, we hope to reduce skin inflammation caused by UVR exposure.

Based on a dose response curve and previously published literature, a dose of 8 μM GSK was added to each cell system 48 h prior to UVR exposure, and 24 h after UVR exposure [28,30,31,39,53]. iROS production normalized to cell viability was measured for each cell line in monoculture, epidermis co-culture, and dermis co-culture systems. Strong NOX2 inhibition was observed in all monocultures and co-culture systems based on reduced iROS levels. The most striking inhibition occurred in the epidermis co-culture, wherein GSK effectively negated the UVR inflammatory response by reducing iROS levels to match those of SHAM levels; reducing the UVBR response by 3-fold and the UVAR+UVBR response by 3.7-fold. Although GSK has been shown to reduce the iROS response in HaCaT cells [28], to our knowledge, this is the first time that GSK has successfully inhibited inflammation in an *in vitro* epidermis model after UVR exposure.

Inspired by the promising reduction in iROS, we analyzed the pro- and anti-inflammatory cytokine secretion with and without GSK treatment. NOX2 has been shown to trigger the NLRP3 inflammasome formation and activation, thus further increasing ROS and inflammation after a stressor, such as sunburn[54]. The NLRP3 inflammasome is an intracellular multiprotein complex that, when activated, produces the secretion of pro-inflammatory cytokines such as IL-1β and IL-18 to eventually induce cell death[55]. Due to the role of NOX2 in activation of the inflammasome complex, we hypothesized that GSK would reduce the secretion of IL-1β. Although GSK reduced iROS 24 h post-UVR, we did not see a significant decrease in IL-1β secretion in our complex skin-immune model. This may be due to IL-1β cytokine secretion peaking outside of our single 24 h timepoint, highlighting a potential limitation of our study. Indeed, Laabei et al., 2025,[55] reported a significant decrease in IL-1 β after only 1 h post-LPS treatment, indicating that our 24 h timepoint may be outside the ideal block of IL-1 β secretion window.

Conclusions

In this work, a baseline biological response to UVR was assessed in two skin-immune systems, including cell viability, intracellular ROS, and cytokine production. Monoculture, epidermal co-culture, and dermal co-culture systems were utilized to evaluate the interactions between immune cells (THP1-PMA and LC) and keratinocytes (HaCaT) 24 h post-exposure to SHAM, 10 J/cm^2 UVA and/or 500 mJ/cm^2 UVBR. We observed a significant cell viability decrease in HaCaT and LC cells when exposed to 500 mJ/cm^2 UVBR, with a significant increase in cytokine production of IL-4, IL-6, IL-1β, and TNFα in the monoculture, in contrast to the cell viability, iROS, and cytokine production of these cells when in an epidermis co-culture model. This interaction highlights the complex skin-immune system interactions necessary to better capture an inflammatory response in skin after a sunburn event. Additionally, we observed cell viability, iROS, and cytokine production in THP1-PMA, LC, and HaCaT cells after exposure to 10 J/cm^2 UVAR. Similar to the UVBR model, our cell lines reacted differently when in a monoculture vs a skin-immune epidermal co-culture and dermis co-culture system, justifying our inclusion of three different cell culture models in our study. Finally, we show that the NOX2 inhibitor, GSK2795039 (GSK), can be used to rescue cell viability and significantly reduce iROS in all cell lines and co-culture systems 24 h post-UVR

exposure. To our knowledge, this is the first time that GSK has been shown to significantly reduce the inflammatory response in a complex skin-immune system.

Materials and Methods

1. Materials

Spontaneously transformed keratinocytes from histologically normal skin (HaCaT) cells were acquired from AddexBio Technologies (San Diego, CA). Human monocytes (THP-1) were acquired from ATCC (Manassas, VA). Phosphate buffered saline (PBS) and trypsin-EDTA for cell culture were obtained from Gibco (Waltham, MA). GSK2795039 (GSK), IL-4, TFG-β, and GM-CSF were purchased from MedChem Express (Monmouth Junction, NJ). CD68 Antibody (eBioY1/82A (Y1/82A)), PE, eBioscience (Cat#12-0689-42), Iscove's modification of DMEM (IMDM) (Cat#12440053), fetal bovine serum (FBS) (Cat#A5670701), RMPI 1640 (Cat#11875093), PrestoBlue HS cell viability reagent (Cat#P50200), H2DCFDA (H2-DCF, DCF) ROS reagent (Cat#D399), and cytokine 10-Plex panel (Cat#LH0001M) were purchased from ThermoFisher Scientific (Waltham, MA) and CD207 (Langerin) antibody FITC was purchased from Miltenyi Biotech (Cat#130-112-367) (Gaithersburg, MD). Phorbol 12-myristate 13-acetate (PMA) and 2-Mercaptoethanol (2-ME) were purchased from Fisher Scientific (Waltham, MA). Transwell experiments used the Corning HTS Transwell-96 permeable support with 0.4 μM PET membrane (Cat#7369) with the HTS Transwell-96 black receiver plate (Cat#3583) (Corning, NY). UV/LED Irradiation Chamber BS-02 from Opsytec Dr. Gröbel GmbH (Ettlingen, Germany). DuoSet ELISA Ancillary reagent kit 1 (Cat#DY007B), Human IL-6 DuoSet ELISA (Cat#DY206-05), Human IL-4 DuoSet ELISA (Cat#DY204-05), Human IL-1 beta/IL-1F2 DuoSet ELISA (Cat#201-05), and Human TNF-alpha DuoSet ELISA (Cat#DY210-05) were acquired from R&D Systems (Minneapolis, Minnesota).

II. Experimental Model and Study Details

1. Cell Culture

HaCaT cells were individually cultured in Iscove's Modification of DMEM (IMDM) medium and supplemented with 10% Fetal Bovine Serum (FBS). THP-1 cells were individually cultured in RPMI 1640 with and 0.05 mM 2-mercaptoethanol, supplemented with 10% FBS. THP-1s were differentiated into THP1-PMA macrophages through the addition of 150 nM PMA to standard THP-1 media for 24 h. Following differentiation, media was replaced with RPMI supplemented with 10% FBS and 2-ME and allowed to rest for 72 h. Differentiation of THP-1 into THP1-PMA macrophages was confirmed with PE-labeled CD68 + via flow cytometry. THP-1 cells were differentiated into Langerhans cell-like dendritic cells through the addition of 100 ng/mL GM-CSF, 25 ng/mL IL-4, and 10 ng/mL TGF-β for 6 days, where media was changed every 3 days. Differentiation of THP-1 into Langerhans cell-like

dendritic cells was confirmed with FITC-labeled CD207 + via flow cytometry. All cells were cultured in standard cell culture conditions (95% relative humidity, 5% CO_2, 37°C).

2. Co-Culture Models

For traditional epidermis co-culture experiments, HaCaT (20k/well) and LC cells (10k/well) were co-cultured together in a black 96-well plates with IMDM media, and allowed to incubate for 24 h. Cells were then exposed to the specific levels of UVR. Following application of UVR, the spent medium was discarded and replaced with fresh medium. For transwell plates, the epidermis layer was set up as described previously, and the THP1-PMA cells (20k/well) were individually cultured in 96-well plates and allowed to incubate for 24 h. Cells were then individually exposed to a specific level of UVR. Following application of UVR, the spent media was discarded and replaced with fresh medium for both the epidermis cells and the THP1-PMA cells. The transwell inserts were then placed into the epidermis cell plate. In experiments with NOX2 inhibitors, cells were pre-treated with 8 μM GSK for 48 h prior to UVR exposure. Upon spent media replacement post-UV radiation, 8 μM GSK was added back to the culture.

3. Cell Viability Determination

Cells were seeded individually in 96-well flat-bottom, black-walled plates. To quantify cell viability, 10% of the total cell media was replaced with the PrestoBlue Viability Assay. Cells were then incubated under standard cell culture conditions for 1 h and fluorescence was measured at Ex/Em = 535/560 nm.

4. Intracellular ROS Determination

Intracellular ROS generated by cells in the presence of UVR and/or NOX2 inhibitors was measured using 2',7'-dichlorodihydroflurescein diacetate H2DCFDA (H2-DCF, DCF) purchased from ThermoFisher (Cat# D399). Cells were plated at a density 80% confluency in black-walled, flat, 96-well plates with or without transwell inserts for co-culture studies. Cells were exposed to buffer (SHAM), UVAR, and/or UVBR and then immediately following UVR treatment cells were incubated under standard cell culture conditions for 24 h. Intracellular ROS was then measured using the kit per manufacturer's instructions together with cellular viability via the PrestoBlue Viability Assay (see above), where Ex/Em = 490/520 nm was used. Fluorescence, normalized to viable cell numbers, for both ROS and cell viability was measured using a SpectraMax plate reader (Molecular Devices, San Jose, CA).

5. Cytokine Panel ELISA Determination

A sandwich enzyme-linked immunosorbent assay (ELISA) was used to quantify cytokines produced by HaCaT, THP1-PMA, and LC-like cells. The cells were seeded in 24-well plates at a density of $2.5x10^5$ cells/mL and allowed to reach 90% confluence. Cells were exposed to SHAM, UVAR, and/or UVBR, and immediately following UVR treatment, the various co-culture models were assembled and all cells were incubated under standard cell culture conditions for 24 h. Post-incubation, the supernatants were collected and levels of pro-inflammatory cytokines (IL-1β, IL-6, TNFα) and anti-inflammatory cytokines

(IL-4) were measured using the DuoSet ELISA Assay Kit (R&D Systems, Minneapolis, MN). ELISA data were analyzed using GraphPad Prism.

6. Luminex Cytokine Panel

The Cytokine 10-plex Human Panel (Invitrogen, Cat# LHC0001M) was used to determine the concentration of GM-CSF, IFN-γ, IL-1β, IL-2, IL-4, IL-5, IL-6, IL-8, IL-10 and TNFα in tissue culture supernatant. Cells were plated at a density 80% confluency in black-walled, flat, 96-well plates with or without transwell inserts for co-culture studies. Cells were exposed to buffer (SHAM), UVAR, and/or UVBR and then immediately following UVR treatment cells were incubated under standard cell culture conditions for 24 h. Experimental groups requiring GSK were treated with 8 μM GSK 48 h prior to UVR, and media was replaced with fresh 8 μM GSK for 24 h post-UVR. Following manufacturer's instructions, 50 μL of spent media was used for the Luminex assay, where only SHAM and the physiologically relevant UVR model were used in the complex skin-immune model (HaCaT + Langerhans cells exposed to UVAR+UVBR, THP1-PMA cells exposed to only UVAR). Data were collected using a Luminex100 system with data acquisition and analysis software. Average result in pg/mL is reported. Limit of detection is noted where applicable.

7. Quantification and Statistical Analysis

One-way ANOVA with Tukey's LSD test for multiple comparisons or t-tests were used for experimental analysis, where noted. All statistical information can be found in the caption of each corresponding figure, including statistical test used, exact value of n. All data are plotted as mean with standard deviation. Data are analyzed and visualized using GraphPad Prism. Symbol meanings: ns $p > 0.05$, *$p \leq 0.05$, **$p < 0.01$, ***$p < 0.001$, and ****$p < 0.0001$.

Declarations

Acknowledgments

The authors would like to acknowledge Nadine Pernodet, PhD, for her contribution to the initial conception of this project and for supporting its funding.

Funding Declaration

This work was supported in part by the Estée Lauder Company.

Author Contributions

J.S.D, J.M.H, and J.S.H conceived the study. R.T.M was responsible for methodology. R.T.M and N.G.A performed data curation, formal analysis, and data visualization. R.T.M., J.S.H., J.S.D wrote the

manuscript. R.T.M., N.G.A., M.S.J., J.S.H., R.K., J.M.H., and J.S.D. reviewed, edited, read, and approved the manuscript and guided the interpretation of the manuscript.

Data Availability Statement

The authors affirm that all data necessary for confirming the conclusions of the article are present within the article, figures, and tables.

Declaration of Interests

The authors declare no competing interests.

References

1. Lotfollahi, Z. The anatomy, physiology and function of all skin layers and the impact of ageing on the skin. *Wound Pract. Res.* **32**, 6–10 (2024).
2. Schwarz, A. et al. Ultraviolet-B-Induced Apoptosis of Keratinocytes: Evidence for Partial; Involvetnent of Tutnor Necrosis Factor-a in the Fortnation of Sunburn Cells. *Soc. Investig dermatology*. **104**, 922–927 (1995).
3. de Szalay, S. & Wertz, P. W. Protective Barriers Provided by the Epidermis. *Int. J. Mol. Sci.* **24**, 1–13 (2023).
4. Yin, H., Hu, M. & Li, D. Regulation of epidermal stratification and development by basal keratinocytes. *J. Cell. Physiol.* **238**, 742–748 (2023).
5. Sharma., H. Y. M. & A. A. O., F. S. *Anatomy, Skin (Integument), Epidermis. StatPearls [Internet]* (StatPearls Publishing, 2025).
6. Wong, R., Geyer, S., Weninger, W., Guimberteau, J. C. & Wong, J. K. The dynamic anatomy and patterning of skin. *Exp. Dermatol.* **25**, 92–98 (2016).
7. Guttman-Yassky, E., Zhou, L. & Krueger, J. G. The skin as an immune organ: Tolerance versus effector responses and applications to food allergy and hypersensitivity reactions. *J. Allergy Clin. Immunol.* **144**, 362–374 (2019).
8. Fukunaga, A. et al. Langerhans Cells Serve as Immunoregulatory Cells by Activating NKT Cells. *J. Immunol.* **185**, 4633–4640 (2011).
9. Ortner, D. et al. Langerhans cells orchestrate apoptosis of DNA-damaged keratinocytes upon high-dose UVB skin exposure. *Eur. J. Immunol.* **54**, 1–10 (2024).
10. Kumar, N. et al. The interplay between cytokines, inflammation, and antioxidants : mechanistic insights and therapeutic potentials of various antioxidants and anti-cytokine compounds. *Biomed. Pharmacother*. **178**, 117177 (2024).
11. Santoro, D. & Boyd, M. The Skin as an Immune Organ. *Diagnostics Ther. Vet. Dermatology*. **1–8** 10.1002/9781119680642.ch1 (2021).

12. Nguyen, A. V. & Soulika, A. M. The dynamics of the skin's immune system. *Int. J. Mol. Sci.* **20**, 1–53 (2019).
13. Phuphanitcharoenkun, S. et al. Characterization of macrophages associated with human skin models exposed to UV radiation. *Commun. Biol.* **7**, 1–13 (2024).
14. Peña, O. A. & Martin, P. Cellular and molecular mechanisms of skin wound healing. *Nat. Rev. Mol. Cell. Biol.* **25**, 599–616 (2024).
15. Tang, X., Yang, T., Yu, D., Xiong, H. & Zhang, S. Current insights and future perspectives of ultraviolet radiation (UV) exposure: Friends and foes to the skin and beyond the skin. *Environ Int* **185**, (2024).
16. IARC Working Group on the Evaluation of Carcinogenic Risks to Humans. Radiation. in Radiation. Solar and Ultraviolet Radiation. IARC Monographs on the Evaluation of Carcinogenic Risks to Humans, (2012).
17. Bennett, S. L. & Khachemoune, A. Dispelling myths about sunscreen. *J. Dermatolog Treat.* **33**, 1–5 (2020).
18. Juzeniene, A. & Moan, J. Beneficial effects of UV radiation other than via viatmin D production. *Dermatoendocrinol* **4**, 109–117 (2012).
19. Salminen, A., Kaarniranta, K., Kauppinen, A. & Photoaging UV radiation-induced inflammation and immunosuppression accelerate the aging process in the skin. *Inflamm. Res.* **71**, 817–831 (2022).
20. Velasco-amador, J. P., Linares-gonzalez, L. & Torre-gomar, F. J. De. Efficacy and Satisfaction of Low Doses UVA1 Phototherapy : A Spanish Experience from a Single Centre. *Life* 13, (2023).
21. Hajialiasgary Najafabadi, A. & Soheilifar, M. H. Masoudi-Khoram, N. Exosomes in skin photoaging: biological functions and therapeutic opportunity. *Cell. Commun. Signal.* **22**, 1–13 (2024).
22. Halliwell, B., Adhikary, A., Dingfelder, M., Dizdaroglu, M. & Division, M. Hydroxyl radical is a significant player in oxidative DNA damage in vivo. *Chem. Soc. Rev.* **50**, 8355–8360 (2021).
23. Chiarelli-neto, O. et al. Inflammatory stimulus worsens the effects of UV-A exposure on J774 cells. *J. Photochem. Photobiol B Biol.* **239**, 112647 (2023).
24. Indo, H. P. et al. A mitochondrial superoxide theory for oxidative stress diseases and aging. *J. Clin. Biochem. Nutr.* **56**, 1–7 (2015).
25. Lam, G. Y., Huang, J. & Brumell, J. H. The many roles of NOX2 NADPH oxidase-derived ROS in immunity. *Semin Immunopathol.* **32**, 415–430 (2010).
26. Noreng, S. et al. Structure of the core human NADPH oxidase NOX2. *Nat. communcations*. 1–11. 10.1038/s41467-022-33711-0 (2022).
27. Korkmaz, H. I. et al. NOX2 Expression Is Increased in Keratinocytes After Burn Injury. *J Burn Care Res. March/Apri*, 427–432 (2020).
28. Li, A. et al. p67phox / NOX2 inhibits psoriasis by regulating the HIF-1 α -glycolysis axis via p53-AMPK in keratinocytes. *Free Radic Biol. Med.* **237**, 503–514 (2025).
29. Fernandes, A., Rodrigues, P. M., Pintado, M. & Tavaria, F. K. A systematic review of natural products for skin applications : Targeting inflammation, wound healing, and photo-aging. *Phytomedicine* **115**,

154824 (2023).

30. Muthukumarasamy, I., Buel, S. M., Hurley, J. M. & Dordick, J. S. NOX2 inhibition enables retention of the circadian clock in BV2 microglia and primary macrophages. *Front. Immunol.* **14**, 1–14 (2023).
31. Li, A. et al. NOX2 deficiency promotes GSDME-related pyroptosis by reducing AMPK activation in neutrophils. *Int. Immunopharmacol.* **143**, 113504 (2024).
32. Otsuka, Y. et al. Differentiation of Langerhans Cells from Monocytes and Their Specific Function in Inducing IL-22–Specific Th Cells. *J. Immunol.* **201**, 3006–3016 (2018).
33. El-Ghorr, A. A. & Norval, M. The role of interleukin-4 in ultraviolet B light-induced immunosuppression. *Immunology* **92**, 26–32 (1997).
34. Qian, M., Fang, X. & Wang, X. Autophagy and inflammation. *Clin Transl Med* **6**, (2017).
35. Yang, J. et al. Targeting Cell Death: Pyroptosis, Ferroptosis, Apoptosis and Necroptosis in Osteoarthritis. *Front. Cell. Dev. Biol.* **9**, 1–18 (2022).
36. Cioce, A., Cavani, A., Cattani, C. & Scopelliti, F. Role of the Skin Immune System in Wound Healing. *Cells* **13**, (2024).
37. Leshem, Y., Levine, A. & Intracellular, R. O. S. *Plant. Signal. Behav.* **103**, 18008–18013 (2006).
38. Stolk, J., Hiltermann, J. N., Dijkman, J. H. & Verhoeven, A. J. Characteristics of inhibition of NADPH Oxidase Activation in Neutrophils by Apocynin, a MEthoxy-substituted Catechol. *Am. J. Respir Cell. Mol. Biol.* **11**, 95–102 (1994).
39. Chen, W. S. et al. Discovery of GSK2795039, a Novel Small Molecule NADPH Oxidase 2 Inhibitor. *Antioxid. redox Signal.* **23**, 358–374 (2015).
40. Guerra, K. & Crane, J. *Sunburn* (StatPearls Publishing, 2025).
41. Danno, K., Toda, K. & Horio, T. Ultraviolet B radiation suppresses mast cell degradulation induced by compound 48/80. *Soc. Investig dermatology*. **0022**, 775–778 (1986).
42. Hu, T. et al. UVB-Induced necroptosis of the skin cells via RIPK3-MLKL activation independent of RIPK1 kinase activity. *CDD Press.* 10.1038/s41420-025-02471-3 (2025).
43. Sugimoto, M., Saitoh, Y., Ichihashi, M. & Miwa, N. Suppressive effects of phosphorylated ascorbate on ultraviolet B radiation-induced DNA damage and differential expression of the wild-type and mutated p53 tumor-suppressor gene in keratinocytes. *Molecualr Med. Rep.* **2**, 917–922 (2009).
44. Pourang, A. et al. Effects of visible light on mechanisms of skin photoaging. *Photodermatol Photoimmunol Photomed.* **38**, 191–196 (2021).
45. Valencia, A., Kochevar, I. E. & Ultraviolet A induces apoptosis via reactive oxygen species in a model for Smith – Lemli – Opitz syndrome. *Free Radic Biol. Med.* **40**, 641–650 (2006).
46. Leong, C. et al. Physiological Doses of Red Light Induce IL-4 Release in Cocultures between Human Keratinocytes and Immune Cells. *Photochem. Photobiol*. **1**, 150–157 (2018).
47. Zhou, L., Jiang, A., Veenstra, J., Ozog, D. M. & Mi, Q. The Roles of Skin Langerhans Cells in Immune Tolerance and Cancer Immunity. *Vaccines* 1–18 (2022).

48. Rose, S. et al. Evidence of oxidative damage and inflammation associated with low glutathione redox status in the autism brain. *Transl Psychiatry*. **2**, 2158–3188 (2012).
49. Miller, C. E. et al. Hydrogen Peroxide Promotes the Production of Radiation-Derived EVs Containing Mitochondrial Proteins. *Antioxid. (Basel)*. **11**, 2119 (2022).
50. Armstrong, D. *Advanced Protocols in Oxidative Stress II* (Springer New York LLC, 2010). 10.1007/978-1-60761-411-1Buffalo.
51. Chettouh-hammas, N. et al. Improvement of Antioxidant Defences in Keratinocytes Grown in Physioxia : Comparison of 2D and 3D Models. *Oxid. Med. Cell. Longev.* 6822931 (2023). (2023).
52. Scordi, I. A. & Vincek, V. Timecourse study of UVB-induced cytokine induction in whole mouse skin. *Photodermatol Photoimmunol Photomed.* **16**, 67–73 (2000).
53. Ijurko, C. et al. Targeting NOX2 and glycolytic metabolism as a therapeutic strategy in acute myeloid leukaemia. *Biomark. Res.* **12**, 1–6 (2024).
54. Sand, J. et al. Expression of inflammasome proteins and in fl ammasome activation occurs in human, but not in murine keratinocytes. *Cell Death Dis* **24**, (2018).
55. Laabei, J. et al. The NOX2-ROS-NLRP3 inflammasome axis in traumatic brain injury. *bioRxiv Prepr* 1–43 (2025).

Figures

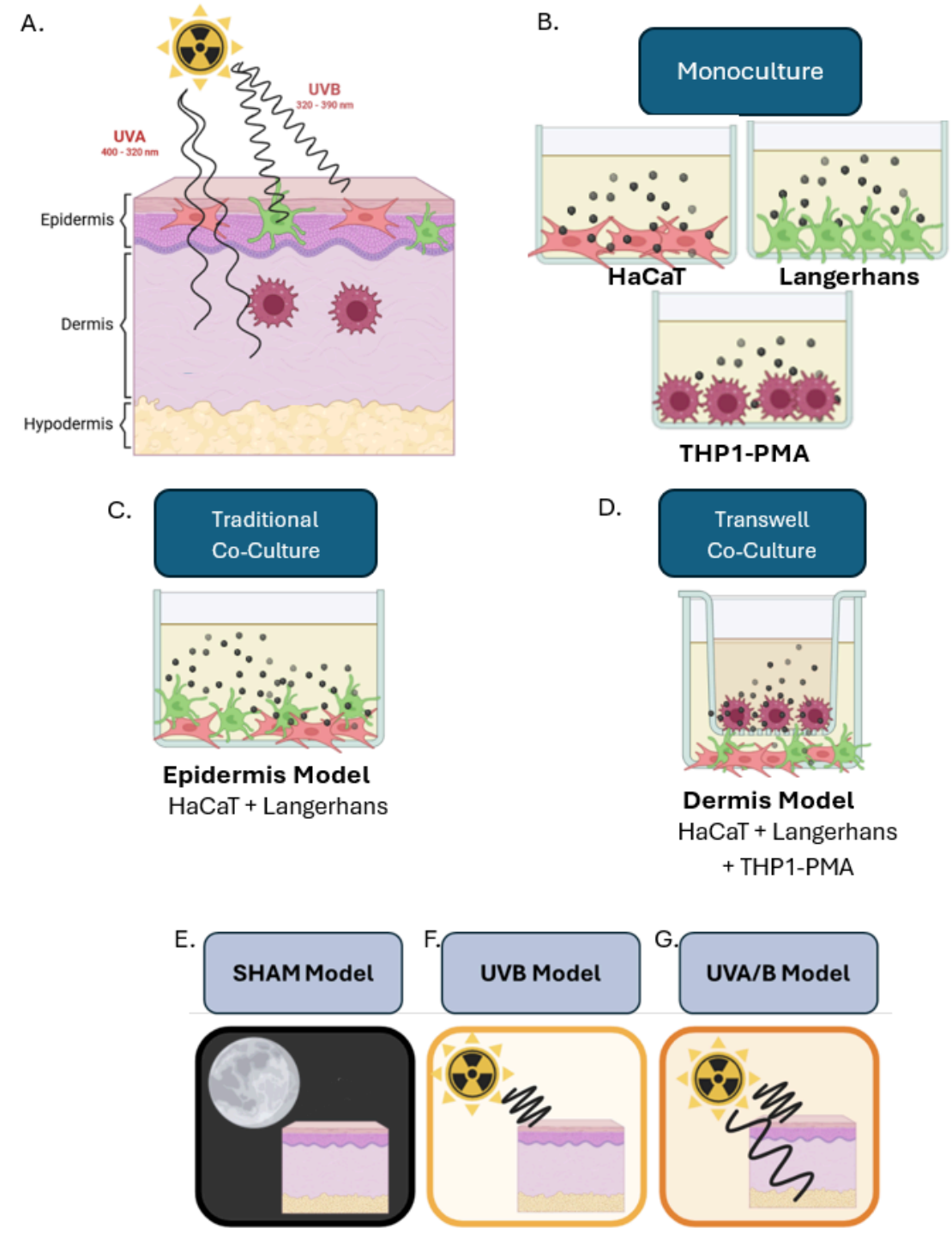

Figure 1. Miceli et al.

Figure 1

Experimental design of mono- and co-culture skin-immune systems. (A) UV and penetration into skin layers. (B) Monoculture cell controls for the three cell types studied, HaCaT, THP1-PMA, and Langerhans cells (LC). (C) Traditional co-culture epidermis model including HaCaT and LC cells. (D) Transwell co-culture of a dermis model of HaCaT, LC, and THP1-PMA cells. An overview of the three UV models used

where a physiologically relevant negative SHAM control group (E), a 500 mJ/cm^2 UVBR control group (F), and a physiologically relevant 10 J/cm^2 UVAR plus 500 mJ/cm^2 UVBR model (G).

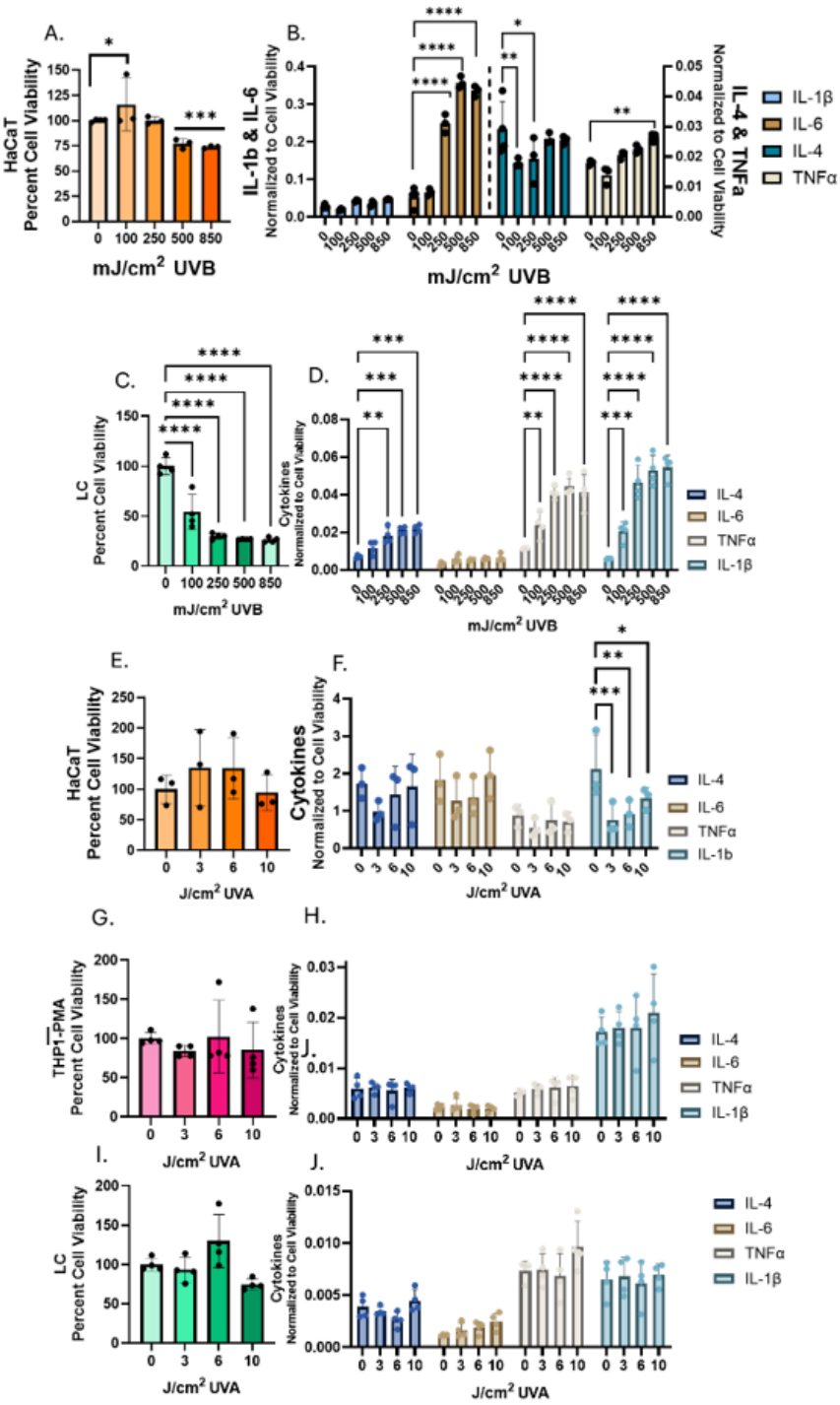

Figure 2. Miceli et al.

Figure 2

Cell viability and cytokine production in HaCaT, THP1-PMA, and LC cells in monocultures after a 24 h exposure to UVR. HaCaT (A, B) and LC (C, D) cells were exposed to 0 - 850 mJ/cm^2 UVBR and cell

viability and cytokines were analyzed 24 h after exposure. HaCaT (E, F), THP1-PMA (G, H), and LC (I, J) cells were exposed to 0 - 10 J/cm^2 UVAR and cell viability and cytokines were analyzed 24 h after UVAR exposure. Doses of 500 mJ/cm^2 UVBR and 10 J/cm^2 UVAR were selected for future experiments. Statistical analysis completed using a one-way ANOVA with a Tukey post-hoc test, where *p<0.05, **p<0.01, ***p<0.001, and ****p<0.0001. N=3 for HaCaT cells. N=4 for THP1-PMA and LC cells.

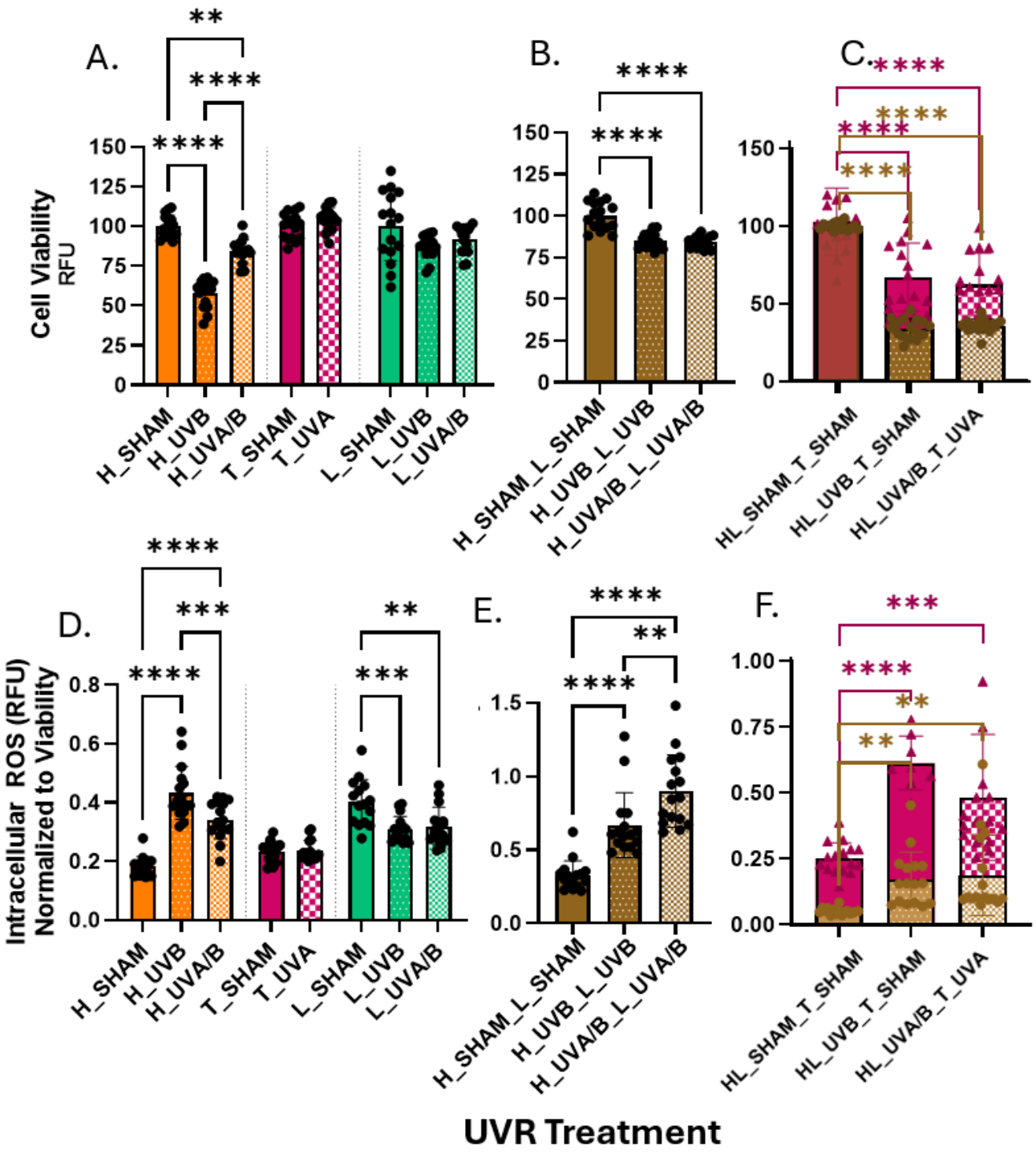

Figure 3. Miceli et al.

Figure 3

Assessment of cell viability (A-C) and intracellular ROS (D-F) production in a complex skin-immune system of HaCaT cells (orange), THP1-PMA macrophages (pink), and LC cells (green). Cell viability in monoculture (A), epidermis co-culture (B), and dermis co-culture (C), and iROS in monoculture (D), epidermis co-culture (E), and dermic co-culture (F) systems 24 h post-exposure to SHAM, 500 mJ/cm^2 UVBR, and/or 10 J/cm^2 UVAR. Statistical analysis completed using a one-way ANOVA with a Tukey post-hoc test, where *p<0.05, **p<0.01, ***p<0.001, and ****p<0.0001. N=16.

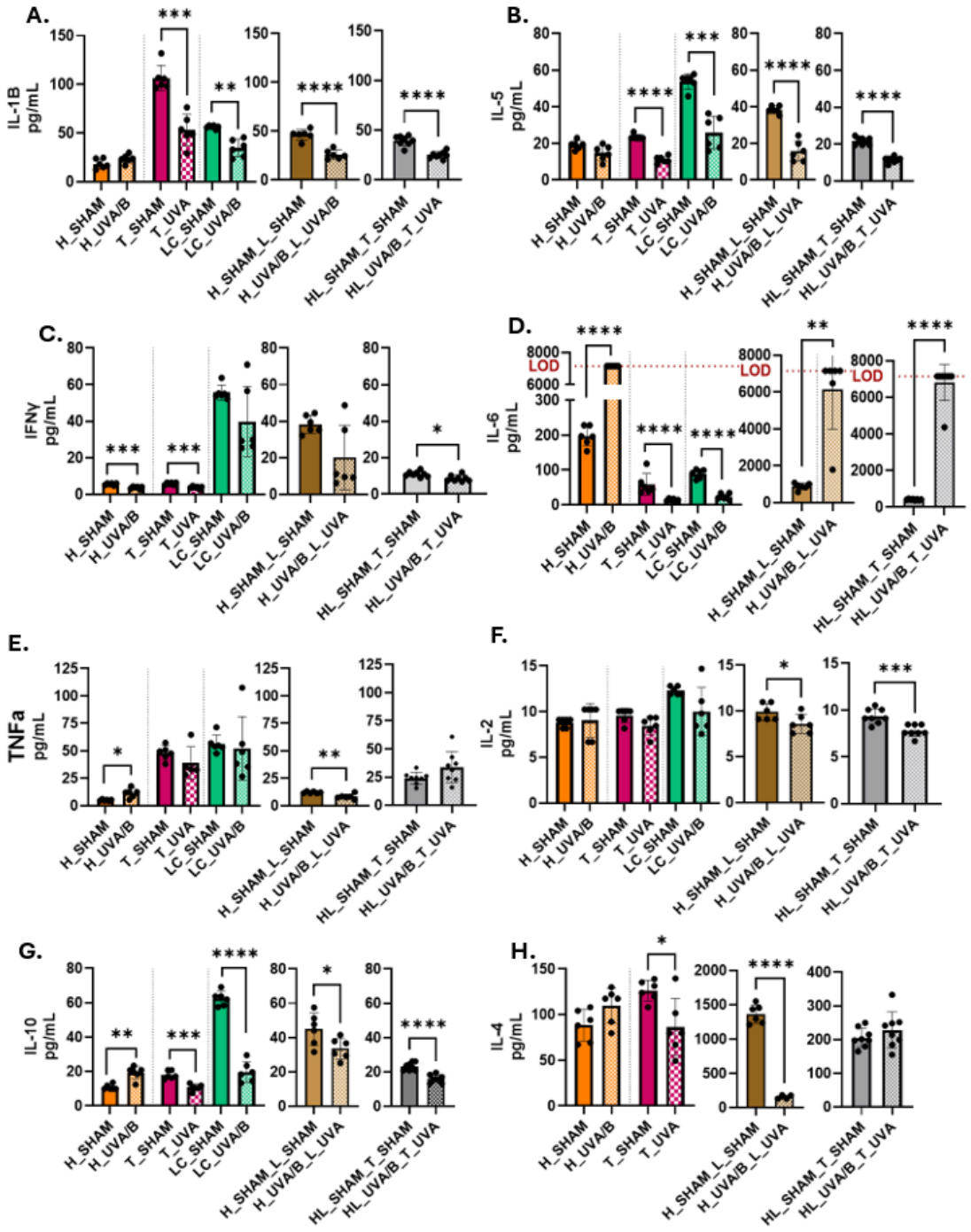

Figure 4. Miceli et al.

Figure 4

Assessment of cytokine production in the complex skin-immune model after exposure to SHAM or UVAR+UVBR conditions. HaCaT cells (orange), THP1-PMA macrophages (pink), LC cells (green), and co-culture epidermis model (brown) and dermis transwell model (grey) are included. Cytokines included are the pro-inflammatory IL-1β (A), IL-5 (B), IFNy (C), IL-6 (D), TNFα (E), IL-2 (F), and the anti-inflammatory IL-10 (G) and IL-4 (H). Cytokines were measured 24 h post-UVR using a Luminex 10-plex kit. LOD refers to the limit of detection specified in the kit via a given standard curve, any data beyond this value is not validated by the standard curve. Statistical analysis completed using t-tests, where *p<0.05, **p<0.01, ***p<0.001, and ****p<0.0001. N = 6.

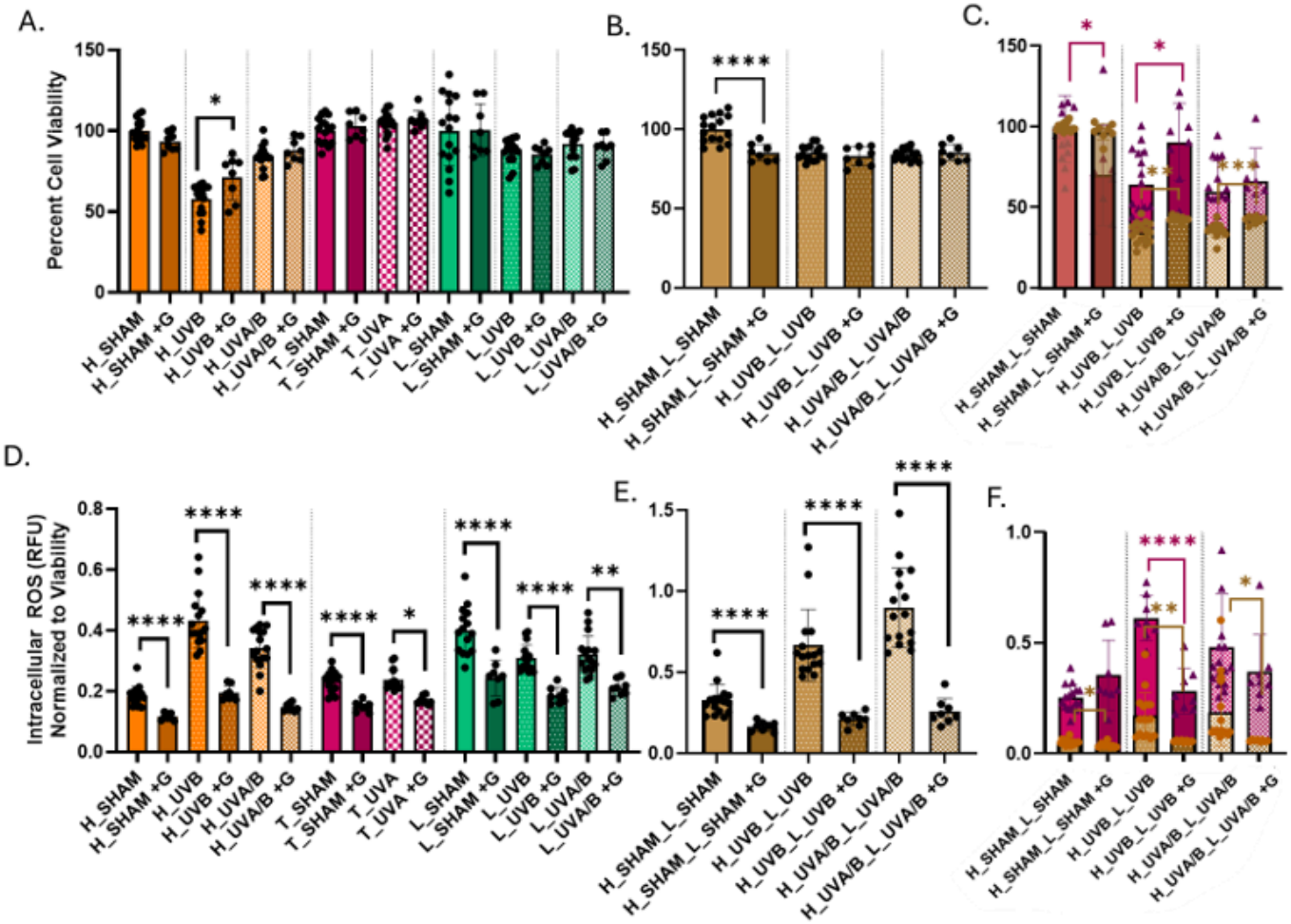

Figure 5. Miceli et al.

Figure 5

Assessment of NOX2 inhibitor, GSK, on cell viability (A-C) and reducing intracellular ROS production (D-F) a complex skin-immune models of HaCaT cells (orange), LC (green), and THP1-PMA (pink) cells. Cell viability in monoculture (A), epidermis co-culture (B), and dermis co-culture (C), and iROS in monoculture (D), epidermis co-culture (E), and dermis co-culture (F) systems 24 h post-exposure to SHAM, 500 mJ/cm^2 UVBR, and/or 10 J/cm^2 UVAR. Statistical analysis completed using a one-way ANOVA with a Statistical analysis completed using a one-way ANOVA with a Tukey post-hoc test, where *p<0.05, **p<0.01, ***p<0.001, and ****p<0.0001. N=16 without GSK treatment, N=8 with GSK treatment.

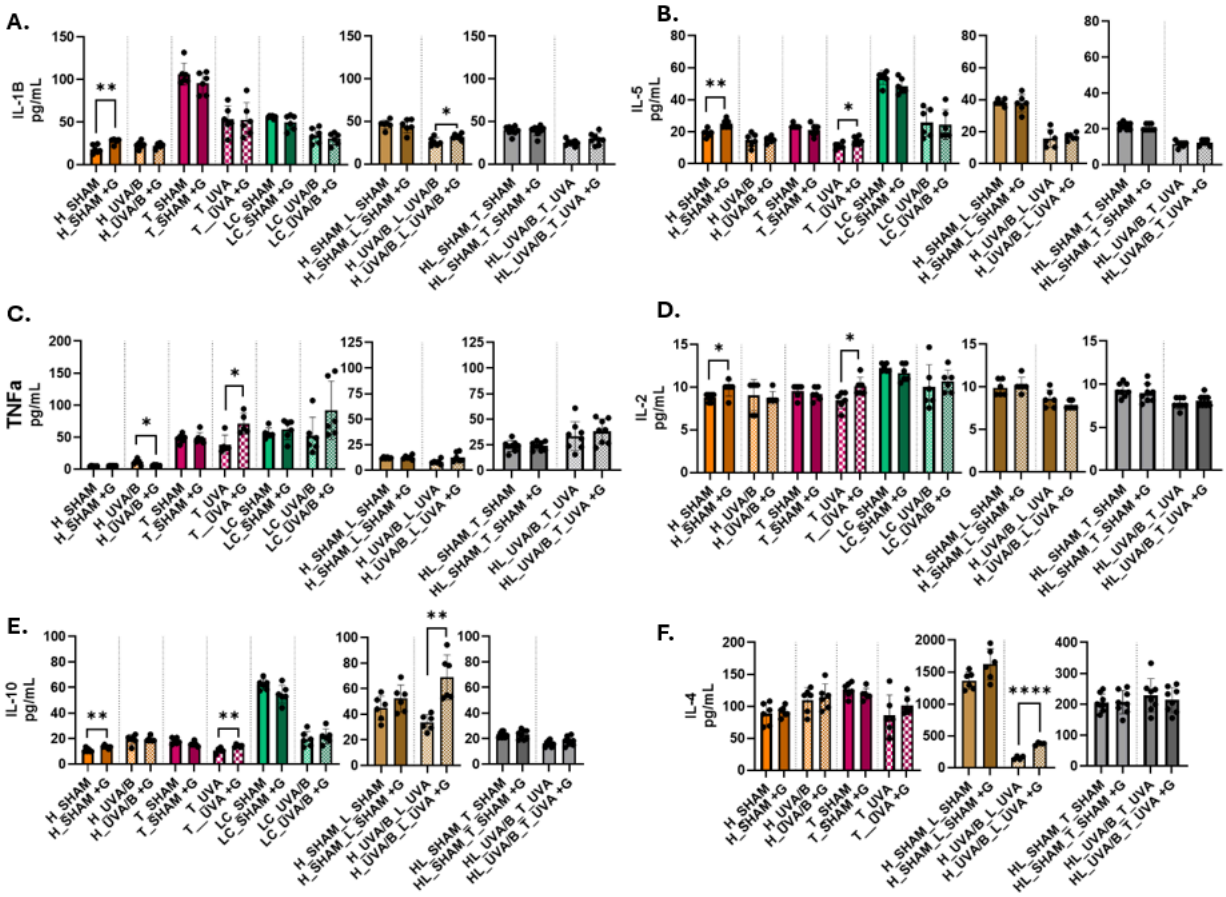

Figure 6. Miceli et al.

Figure 6

Assessment of NOX2 inhibitor, GSK, on cytokine response in the complex skin-immune model, 24 h post SHAM or UVAR+UVBR exposure. HaCaT cells (orange), THP1-PMA macrophages (pink), Langerhans-like cells (green), and co-culture epidermis model (brown) and dermis transwell model (grey) are included. Cytokines included are the pro-inflammatory IL-1β (A), IL-5 (B), the pro-/anti-inflammatory TNFα (C), IL-2 (D), and the anti-inflammatory IL-10 (E) and IL-4 (F). Cytokines were measured 24 h post-UVR using a Luminex 10-plex kit. Statistical analysis completed using t-tests, where where *p<0.05, **p<0.01, ***p<0.001, and ****p<0.0001. N = 6.

Supplementary Files

This is a list of supplementary files associated with this preprint. Click to download.

- Micelietal.SupplementalDataSciReports.docx